Mon. Not. R. Astron. Soc. **286,** 604–616 (1997)

High-resolution spectroscopy of Vega-like stars – I. Effective temperatures, gravities and photospheric abundances

S. K. Dunkin,[1] M. J. Barlow[1] and Sean G. Ryan[2]
[1]*Department of Physics and Astronomy, University College London, Gower Street, London WC1E 6BT*
[2]*Anglo-Australian Observatory, PO Box 296, Epping, NSW 2121, Australia*

Accepted 1996 October 30. Received 1996 October 21; in original form 1996 April 9

ABSTRACT

Vega-like stars are young main-sequence stars exhibiting an excess emission of infrared radiation. Modelling this excess depends not only on the parameters assigned to the grains, but on those assigned to the stars themselves. In an effort to update and improve the information available on this class of star, we have analysed 13 stars classed as Vega-like, having an infrared excess attributable to dust emission, along with two spectral standards which have also been found to show excess emission from dust. In this, the first of two papers, we derive stellar properties (spectral type, effective temperature and log g) and photospheric abundances.

The spectral types derived revealed that one of the sample was a luminosity class III giant, ruling it out of the Vega-like class, and two others underwent a significant reclassification. The remainder had their type confirmed. All but two programme stars have been found to be emission-line stars – their emission-line properties are discussed in Paper II.

Attention has recently been drawn to the possible link between Vega-like stars and the photospheric metal-depleted class of A-type stars, the λ Boötis stars. These latter stars are hypothesized to have obtained their underabundances by the accretion of depleted circumstellar gas on to the photosphere of the star. Since Vega-like stars are expected to have discs of dust, it might be expected that accretion may cause this same phenomenon. We have analysed four A-type stars in our sample and two A-type standards, deriving photospheric abundances for up to 10 elements. No pattern of underabundance similar to λ Boötis stars was found, although a depletion of silicon was found in two stars (up to 0.86 dex below solar) and of magnesium in one star (0.56 dex lower). The depletion could be attributable to the accretion of those elements on to grains in the circumstellar environment of these stars.

Key words: stars: abundances – stars: fundamental parameters – stars: pre-main-sequence.

1 INTRODUCTION

During a calibration scan of the photometric standard star α Lyr (Vega), the *Infrared Astronomical Satellite* (*IRAS*) detected excess flux at wavelengths centred at 25, 60 and 100 μm, above that expected of a blackbody at the temperature of the star (Aumann et al. 1984). During the course of the mission three other bright main-sequence stars were found to exhibit this infrared (IR) excess: α PsA (Fomalhaut), ϵ Eri and β Pic which, together with Vega, had additional, pointed observations made to obtain accurate photometry (Gillett 1986). Together, these four stars have become known as the prototypes of the 'Vega-like' phenomenon. Subsequent searches of the *IRAS* data base (e.g. Aumann 1985; Walker & Wolstencroft 1988) have since expanded the known membership of the class significantly. The excess emission from these main-sequence stars has been attributed to circumstellar material in the form of a disc or ring of dust, similar to that postulated for our own Solar system. Aumann et al. (1984) demonstrated that the excess in α Lyr could be modelled using an 85-K blackbody, and suggested that the most plausible explanation of this was the presence of dust in the circumstellar environment which was left over from the original protostellar cloud from which it formed.

The accretion of dust-depleted gas from the circumstellar environment on to the stellar surfaces has been proposed as an explanation of the λ Boötis phenomenon (Venn & Lambert 1990). λ Boo stars are chemically peculiar A-type stars, exhibiting underabundance in elements such as magnesium, calcium and iron. In terms of the accretion hypothesis, King (1994) investigated the possible link between the λ Boo phenomenon and Vega-like stars, with inconclusive results. In Section 4 we further investigate such a link by carrying out an abundance analysis of a sample of A-type Vega-like stars. Paper II (Dunkin, Barlow & Ryan 1997) goes on to

Table 1. The programme stars observed and their spectral classification. The errors on the spectral types derived from this work are ±2 subclasses for the stars where suitable standards were not observed by us (HD 2623, 23362 and 135344) and ±1 subclass for the remainder of the sample.

Star		Name	Prev Class	Ref	This work	Site	Date of
HD	SAO						obs.
2623	109235		K2	(2)	M2III	OAN	26 Sept 93
23362	111388		K2	(2)	K2V	OAN	26 Sept 93
35187	77144		A2/3 IV/V	(3)	A2/3 IV/Ve	OAN	26 Sept 93
98800	179815		K5V	(4)	K5Ve	AAT	25 Feb 94
123160	158350		K5	(2)	G5V	AAT	20 June 94
135344	206462		A0V	(5)	F4Ve	AAT	25 Feb 94
139614	226057		A7V	(5)	A7Ve	AAT	20 June 94
141569	140789		A0Ve	(8)	A0Ve	AAT	20 June 94
142666	183956		A8V	(7)	A8Ve	AAT	20 June 94
143006	183986		G5e	(9)	G5Ve	AAT	20 June 94
144432	184124		A9/F0V	(6)	A9/F0Ve	AAT	20 June 94
158643	185470	51 Oph	B9.5V	(10)	B9.5Ve	AAT	20 June 94
169142	186777		B9V	(6)	A5Ve	AAT	17 June 94
Spectral Standards							
161868	122754	γ Oph	A0V	(11)	–	AAT	20 June 94
187462	87766	α Aql	A7V	(11)	–	AAT	20 June 94
198001	144810	ϵ Aqr	A1V	(11)	–	AAT	20 June 94
200499	189986	22 Cap	A5V	(11)	–	AAT	16 June 94
214850	108094		G3V	(11)	–	AAT	16 June 94
216956	191524	α PsA	A3V	(1)	–	AAT	16 June 94

References:
(1) = SIMBAD database,
(2) = Henry Draper Catalogue,
(3) = Zuckerman, Forveille & Kastner (1995),
(4) = Fekel & Bopp (1993),
(5)–(7) = Michigan Spectral Catalogue, vols 2–4 (Houk 1978, 1982, 1988),
(8) = Andrillat, Jaschek & Jaschek (1990),
(9) = van der Veen, Trams & Waters (1993),
(10) = Bright Star Catalogue (Hoffleit & Jaschek 1982),
(11) = Danks & Dennefeld (1994).

discuss the ages of the stars, as determined by lithium abundances in the later-type stars and the emission-line activity levels of the stars, together with their possible relationship to the Herbig Ae/Be stars. Circumstellar absorption lines are also investigated in Paper II.

2 OBSERVATIONS

Optical echelle spectra were obtained at two sites. The majority of the data were obtained at the Anglo-Australian Telescope (AAT) using the UCL echelle spectrograph. The 31.6 g mm^{-1} echelle and the 1024 × 1024 pixel Tektronix CCD detector were used with slit widths varying between 1 and 1.5 arcsec when aquiring the data on the nights of 1994 June 16/17/20, and 1994 February 25. Additional data were obtained by Dr Francisco Diego (UCL) with the 2.1-m telescope at the Observatorio Astronomico Nacional (OAN), San Pedro Martir, Mexico on 1993 September 26. The data were obtained during a commissioning run of the ROESC echelle spectrograph, using a slit width of 2 arcsec and a 1024 × 1024 pixel Thomson CCD. From the measured full-width at half maximum (FWHM) of comparison thorium–argon arc lines, the resolving powers of the AAT and OAN spectra were found to be ($R \equiv \lambda/\Delta\lambda$) ~ 44 000 and 15 000 respectively. The signal-to-noise ratio (SNR) for the AAT data was typically 200:1, and that of the OAN data 150:1. The wavelength coverage of the OAN data was 4100 to 8700 Å, complete from 4100 to 6600 Å and with gaps between the orders for the remaining portions of the spectrum. The AAT data were taken at two wavelength settings, blue and red. The blue spectra gave complete coverage from 3800 to 4960 Å and the red spectra incomplete coverage between 5260 and 9200 Å.

The programme stars listed in Table 1 were selected mainly from the list of Walker & Wolstencroft (1988), with the remainder coming from the list of Stencel & Backman (1991). The wavelength settings of the AAT observations were chosen to include as many lines as possible from those studied by Venn & Lambert (1990) in their study of the λ Boötis phenomenon. The settings also covered the lines of Ca II K and Na I D (important for spectral classification and the study of circumstellar material), Hα (to study circumstellar emission around the stars) and the Li I line at λ6708 Å (as an age indicator for the cooler stars).

Several spectral standard stars were also observed at the same time as the programme stars, and these are tabulated along with the programme stars in Table 1. The standards were selected from the list of Danks & Dennefeld (1994). Most of the stars had previously been observed at infrared, mm and submm wavelengths by Sylvester, Barlow & Skinner (1992) and Sylvester et al. (1996).

During the course of their work, it was realized that spectral classification from optical data was generally lacking for these stars, and a wish to improve the situation was the main reason for initiating this work.

3 SPECTRAL CLASSIFICATION

The classification of stars remains one of the most powerful tools in astronomy. The modern classification system was first introduced by Morgan, Keenan & Kellman over 50 years ago (Morgan, Keenan & Kellman 1943), and covered the wavelength region 3900–4900 Å. This original (MKK) atlas was subsequently revised in 1953 (Johnson & Morgan 1953) and in 1973 (Morgan & Keenan 1973: referred to as the 'Revised MK'). Traditionally, spectral classification has been attempted in the blue region of the optical spectrum, quite possibly because of the sensitivity of the first detectors used, such as photographic emulsions, but also because of the wealth of lines available for study in this area. More recently the classification system has been extended to include other wavelengths (e.g. Abt et al. 1968, see also Torres-Dogden & Weaver 1993). The MK classification system takes account of the blue-region spectral features and utilizes an atlas of standard stars with which to compare the programme stars. Certain spectral features, lines and bands (spectral criteria) are used that are particularly sensitive to temperature and luminosity class, and act as guidelines in the process of spectral classification. As an example, references to the more commonly used spectral criteria can be found in Jaschek & Jaschek (1990).

Table 1 lists the spectral types of the programme stars and spectral standards used in this work. Column 4 indicates the previous spectral type assigned to the star, with column 6 giving the results of the present work.

Only standards of A type, plus one G3V-type standard star, were observed along with the programme stars. These were used where possible for classification purposes. Allen & Strom (1995) have published a set of standard F-, G-, K- and M-type stars at 6-Å resolution between 5600 and 9000 Å and made them available via anonymous ftp. Their classification method involved utilizing relations by Schmidt-Kaler (1982) and others to convert absolute magnitudes to spectral types. We made use of these data in the absence of suitable standards from our own sample.

3.1 Temperature classification

Although the MK classification system is based on more than just the estimation of a few lines, using the entire blue region of the optical spectrum to compare with standard stars, a few lines and blends have been identified that are particularly useful in determining spectral class. Gray & Garrison (1987, 1989a,b) and references therein quote: the strength of the Ca II K line, the strength of several metallic lines and blends (which are particularly prominent in the visible region of spectra) and the hydrogen lines as the main criteria for classifying A- to F-type stars. For G-type stars the spectra become more complicated. Hydrogen is weak, metallic lines are numerous and bands of CN and CH become visible. The Ca I line at λ4226 becomes temperature sensitive and can be used in ratio with other lines. Once the K-type stars are reached, molecular bands of CH become apparent with TiO seen in K5 and later-type stars which can be used as excellent indicators of temperature. The same is valid for M-type stars, where bands of VO are also seen.

In determining spectral types, the classifier must be sure that there are no anomalies in the abundances of the star. The programme stars were analysed for evidence of non-solar abundances, and in general elements that are particularly sensitive to underabundance phenomena (i.e. Mg and Ca, see Section 4) were excluded from the classification process.

For most of the programme stars, classifications could be assigned by studying the line strengths of the stars in comparison with the standards observed. In general, the metallic lines in the 3900–4900 Å range were used for the A-type stars, with other features mentioned above being used for the later-type stars. Where necessary, spectra were artificially broadened to obtain similar $v \sin i$ values for a more accurate comparison with standards of higher rotational velocity or the spectra were degraded to match the resolution of spectra in work by other authors.

Table 1 shows that the majority of the programme stars had their previous spectral type confirmed, although there are four notable exceptions to this. HD 169142 (Fig. 1) is now found to be six subclasses cooler than indicated by its original classification of B9V in the Michigan Spectral Catalogue. By comparison with spectra of an A5V MK standard, it is found that HD 169142 has an A5 type. HD 169142 also shows no discernible He I lines at λλ4026 and 4471, which are present in B stars. Various spectral regions of these stars were also artificially broadened to the $v \sin i$ of the fastest rotator of other standards and compared again. Overall, the A5 classification of HD 169142 was confirmed. HD 123160 (Fig. 2) appears to be a G5 rather than a K5 star. This classification was made by comparing line strengths with the G3V standard in our sample and the G5V target star HD 183986. HD 135344, originally classified as A0 in the Michigan Spectral Catalogue, has recently been reclassified as F4Ve (Oudmaijer et al. 1992), F8V (Coulson & Walther 1995) and F6V (Zuckerman et al. 1995). From our spectra of this star, it is clear that it is far cooler than the A0 class originally assigned to it. Its spectral features are certainly closer to late A type than early G, therefore favouring the classification obtained by Oudmaijer et al. of F4Ve. We also degraded the spectra of this star to the resolution used by Allen & Strom and made a comparison with their spectra. The comparison seems to suggest that an F4V classification is valid. HD 2623 was originally classified as a K2 star in the Henry Draper Catalogue. However, our spectra show that the star is of much later type, judging by the presence and strength of the TiO bands in its spectrum. The star will be discussed further in the next subsection in the light of its luminosity class.

3.2 Luminosity classification

For some spectral types, changes in line strengths due to luminosity differences can be subtle. Because of this, line ratios are generally used for luminosity classification, and the ratios that are more commonly used are listed in Table 2.

It should be noted that the line ratios quoted in Table 2 have been obtained at several different resolutions and therefore some may be more suitable than others depending on the resolving power of the instrument used. The resolution of our spectra is far higher than that normally used for pure spectral classification work. Where possible we have classified our stars by comparison with the standards we obtained at the same resolution or degraded our spectra to appropriate resolutions to compare line ratios and spectral features with the previously published work of others. Possible abundance anomalies in the stars could render some of the ratios quoted unusable. The table does, however, give some indication of the lines most commonly used for the determination of the luminosity classes of stars.

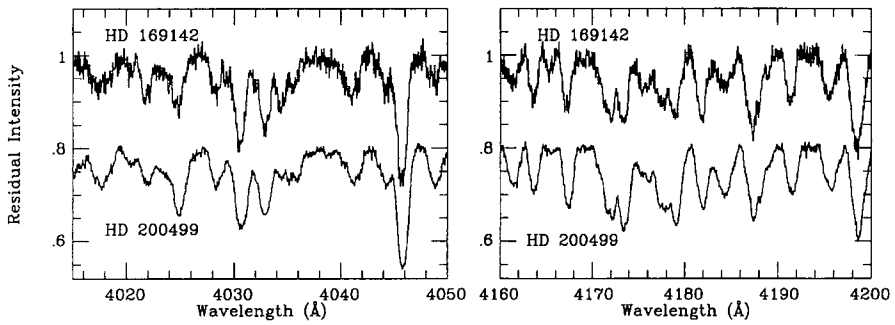

Figure 1. Originally classified as a star of B9 type, HD 169142 can be seen to exhibit the characteristics of an A5 star when compared with the A5V standard, HD 200499.

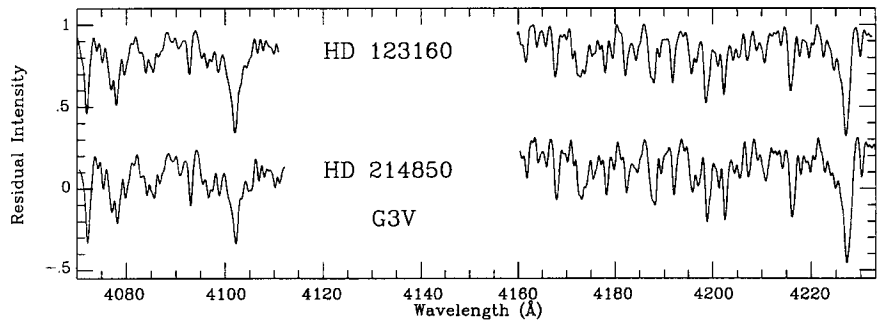

Figure 2. HD 123160 had originally been classified as a K5 star (HD catalogue), however the appearance and strength of lines in its spectrum suggest it is of G3 or G5 type when compared to the G3V standard, HD 214850.

Table 2. Line ratios used for the luminosity classification of stars. 'Positive luminosity effect' indicates an increase in the line/ratio with increasing luminosity and vice versa.

Type	Ratio	Effects	Ref.
A0	H line profiles		1.
Early A	Stark wings	β index highest for dwarfs	2.
A5	Fe II λλ 4417 / Mg II λ 4481	Positive luminosity effect	1.
To A7	Fe II, Ti II, Cr II λλ 4172-4179 / Fe II λ 4203	Positive luminosity effect	2.
Early F	Fe II, Ti II, Cr II λλ 4172-4179 / λ 4271	Positive luminosity effect	3.
	λ 3983 / λ 4005		3.
	λ 4023 / λ 4005		3.
F (general)	Ti II λ 4444 / Mg II λ 4481		4.
	Fe I λ 4071 / Sr I λ 4077	Sr increases for higher luminosity	4.
	Sr II λ 4077 / Fe I λ 4045	Sr increases for higher luminosity	4.
	Sr II λ 4077 / H I λ 4100	Sr increases for higher luminosity	4.
G	Sr II, Fe λ4216 / Ca I λ 4226		4.
	Sr II λ4077/ Fe λ 4063, 4071		4.
G8-K5	Mg I λλ 5167-72-83		4.
K	Sr II λ4077 / Fe I λλ4061,71		4.
	Sr II, Fe λ4216/ Ca I λ 4226		4.
M	Ca I	Negative luminosity effect	4.
	Continuum(λ7035±30 Å) / Ca H (λ6975±30 Å)	Negative luminosity effect	5.
	Continuum(λ8575±10 Å) / Ca II (λ8542±10 Å)	Positive luminosity effect	5.

References: (1) Morgan, Abt & Tapscott (1978), (2) Gray & Garrison (1987), (3) Gray & Garrison (1989a), (4) Jaschek & Jaschek (1990), (5) Kirkpatrick, Henry & McCarthy (1991).

Table 3. Table of absorption-line equivalent widths for the programme and standard A-type stars in our sample. All values in mÅ, except Ca II, in Å. The ↓ sign indicates a combined equivalent width, due to the blending of the lines.

		Star (see notes)											
		1	2	3(S)	4(S)	5	6(S)	7(S)	8	9(S)	10	11	12
$v \sin i$ (km s^{-1})		267	236	214	95	93	88	52	55	189	24	70	74
Spectral Type		A0	A0	A0	A1	A2/3	A3	A5	A5	A7	A7	A8	A9/F0
Species	λ(Å)												
Mg II	4481.13	380	360	370	414	428	628	548	313	495	340	472	723
	4481.33	↓	↓	↓	↓	↓	↓	↓	↓	↓	↓	↓	↓
Ca I	4226.73	94	141	49	165	670	402	408	409	499	485	561	560
Ca II	3933.66	1.00	0.48	0.69	1.19	–	2.29	3.31	2.50	4.16	3.04	3.87	5.30
Ti II	4012.37	43	–	33	68	–	141	98	82	140	130	124	167
	4290.22	83	81	18	144	257	343	322	278	333	275	491	552
	4443.80	124	42	–	125	279	369	210	182	341	62	485	362
	4468.49	83	–	161	–	218	–	289	192	–	203	322	404
	4501.27	84	51	63	119	129	189	164	153	151	188	212	248
	4533.97	111	63	86	180	229	269	285	192	352	245	272	341
	4563.76	51	–	37	125	188	212	173	129	149	181	226	284
	4571.97	56	–	165	125	181	201	197	158	137	209	229	285
Fe I	3920.26	21	–	24	36	–	–	157	175	56	180	249	192
	3922.91	25	–	16	26	–	108	–	141	–	193	182	193
	3930.30	–	–	–	–	–	219	106	150	–	173	143	185
	3997.39	96	–	19	78	–	269	257	236	288	166	381	426
	4005.25	82	–	55	122	–	350	262	212	362	277	344	373
	4045.82	42	109	97	138	–	346	315	300	305	317	372	466
	4063.60	88	40	22	121	–	257	191	205	215	272	268	456
	4071.74	–	–	80	92	–	231	–	204	28	223	294	431
	4202.03	60	–	15	114	–	173	143	171	129	211	199	188
	4235.94	78	–	7	192	147	129	134	136	72	169	187	317
	4260.48	164	–	27	61	164	–	235	187	225	236	277	307
	4282.41	41	–	34	–	127	–	103	165	–	138	216	297
	4466.55	42	–	7	–	48	–	74	92	–	104	74	126
Fe II	4233.17	86	–	84	192	245	303	259	238	363	336	348	426
	4472.92	46	–	4	–	57	–	54	31	–	47	–	221
	4508.28	74	–	54	102	125	171	125	87	134	150	167	209
	4515.34	74	21	26	89	90	162	123	105	106	132	146	168
	4520.23	28	52	4	195	151	259	112	88	30	129	115	118
	4522.63	54	↓	28	↓	↓	↓	162	128	64	168	180	169
	4541.52	66	78	87	60	78	125	102	69	92	75	132	183
	4576.33	24	–	68	66	28	112	77	59	–	86	96	137
	4582.84	85	–	13	146	186	321	12	164	60	63	234	290
	4583.83	↓	–	36	28	↓	↓	236	↓	115	193	↓	↓
	4629.34	71	50	40	19	82	180	156	109	–	150	175	227
Sr II	4077.71	117	–	48	89	–	351	279	176	253	262	328	458
	4215.52	42	10	–	81	299	211	215	215	199	275	282	309

Notes to Table 3.

1 = HD 158643
2 = HD 141569
3 = HD 161868
4 = HD 198001
5 = HD 35187
6 = HD 216956
7 = HD 200499
8 = HD 169142
9 = HD 187462
10 = HD 139614
11 = HD 142666
12 = HD 144432

(S) denotes that the star is an MK standard.

In the case of early A-type stars, the Stark wings of the hydrogen lines are an excellent indicator of luminosity class. The Strömgren β index, which measures the strength of the Hβ line and hence the development of the Stark wings, can be a measure of the luminosity in these stars and Gray & Garrison (1987) present a table (their table 5) correlating the β index with luminosity class for high (>150 km s^{-1}) and low (<150 km s^{-1}) $v \sin i$ stars. We have compared the β indices of our sample of early A-type stars (B9.5–A2 inclusive) with the mean β-index calibration of GG1. We obtained the β indices of our stars from the catalogue of Hauck & Mermilliod (1990). The value for the A0 star HD 141569 corresponded to that of luminosity class V (the standard HD 161868 was also used to validate the result and was found to correspond to its correct luminosity class). However, the β indices of HD 158643 (51 Oph) and HD 35187 did not correspond to those of a dwarf. Both 51 Oph and HD 35187 are emission-line stars (e.g. Paper II), 51 Oph showing emission in Hβ and HD 35187 exhibiting variable emission. These facts may well have affected the measurement of the β indices. In light of this, we adopt the luminosity classes of these stars from the literature (as outlined in Table 1).

The luminosity classes of the remainder of the A-type stars and the later F-, G- and K-type stars in our sample were classified using suitable ratios from those listed in Table 2. Inspection of the spectrum of HD 2623 reveals it to be of luminosity class III, a giant. This had previously been suspected by Whitelock et al. (1991) who noted that the *JHKL* colours of this star were more consistent with a giant of spectral type M3–M5. Since our concerns lie only with main-sequence or pre-main-sequence stars, HD 2623 will not be considered further in the remainder of the paper. In summary, the luminosity classes of stars of spectral type A5 and later were classified according to line ratios, the A0Ve star HD 141569 from a β-index calibration in GG1, and those of HD 35187 and 158643 (51 Oph) were adopted from the literature.

4 ABUNDANCE ANALYSIS OF THE A-TYPE STARS

In recent years, there has been increased interest in the group of stars known as the λ Boötis stars. These are chemically peculiar stars, usually A-type, with typical rotational velocities of ~100 km s^{-1} (King 1994), as are typical of stars of that type (Gray 1988). The spectra are characterized by weak metallic lines, and some elements can be underabundant by up to a factor of 100 compared with solar values (Venn & Lambert 1990, hereafter referred to as VL90). Explanations of the observed underabundances have been advanced in terms of diffusion in the presence of mass loss (Michaud & Charland 1986), and accretion of depleted interstellar gas on to the photosphere (VL90; Charbonneau 1991; King 1994). In the case of A-type stars, radiation pressure is hypothesized to prevent dust grains (but not gas atoms) from accreting on to the stellar surface. According to this hypothesis (VL90; Waters, Trams & Waelkens 1992), the λ Boötis phenomenon should be confined to A-type stars because hotter B-type stars ionize the circumstellar gas, with radiation pressure then preventing both gas and dust from accreting, while the possession of a surface convection zone by F-type and cooler stars prevents the formation of a thin photospheric layer with the abundance distribution of the accreted circumstellar gas.

The accretion theory is of particular interest to this study; King (1994) studied the link between A-type stars of λ Boo type and those having IR excesses. He found that < 20 per cent of stars in his λ Boo catalogue had *IRAS* excesses. However, the fraction of λ Boo stars with circumstellar dust could be much higher – King argued that the amount of accreted depleted gas required to reproduce the λ Boo phenomenon is so small that associated dust will not necessarily be detectable at IR or submm wavelengths. Nevertheless, the positive identification of other Vega-like stars as λ Boo stars would strengthen the accretion hypothesis. In light of these arguments we carried out abundance analyses of the A-type stars of our sample.

Table 4. Expected equivalent widths of some lines in A-type stars, in mÅ. Taken from Jaschek & Jaschek (1990).

Type	Ca II K	Fe I λ4045	Sr II λ4077
A0	300	100	100
A3	210		
A5	350	200	
A7	450		
F0	650	300	200

4.1 Initial inspection

VL90 measured the equivalent widths of many lines in selected λ Boo stars (their table 2) to determine any underabundances present in the stars. They converted their equivalent widths to abundances using the program WIDTH6 and a model atmosphere selected from the grid used by Baschek & Slettebak (1988) and computed by them using the program ATLAS6 (Kurucz 1979). Where this method was not possible due to blending of lines, they computed a synthetic spectrum using the program MOOG (Sneden 1973) and matched it to an observed spectrum.

Where possible, the lines analysed by VL90 were also measured in our spectra to qualitatively indicate the presence of depleted species (Table 3). The equivalent widths of the lines were determined using the DIPSO software package available at the UCL Starlink node (Howarth & Murray 1988). Based on a comparison of equivalent widths alone, no major (0.5–2 dex) underabundances such as might be expected in λ Boo stars were found, with two exceptions in Mg (see Section 4.4). The absolute measurement of the equivalent widths in Table 3 should be treated with caution. The high $v \sin i$ of a number of stars made it almost impossible to

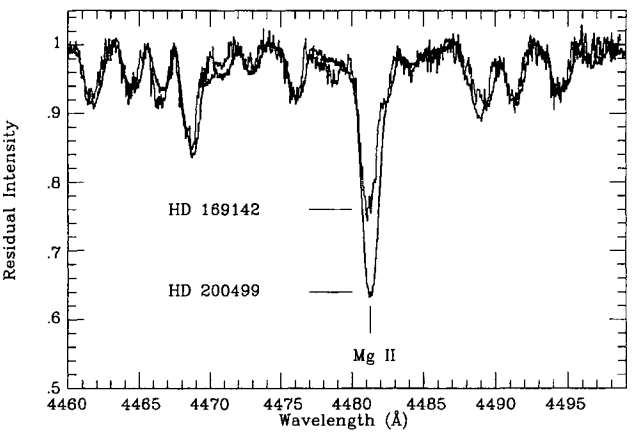

Figure 3. Thin line – HD 169142, thick line – A5V standard (HD 200499). The underabundance of magnesium in HD 169142 is clear. See text for details.

measure just the single line required. For this reason, the equivalent widths measured for some stars are higher than those generally expected for stars of a particular spectral type (see Table 4). However, because the comparison included measurements of the standards in our sample, relative comparisons within our sample could be made before looking at the data of VL90.

Comparisons between standards and programme stars showed clearly the largest of the depletions, as illustrated in Fig. 3. Here the line of Mg II at λ4481 is shown in the spectrum of HD 169142 together with that of a standard of the same spectral type and similar $v \sin i$ (HD 200499). The weakness of the Mg II line in HD 169142 relative to HD 200499 is clear. Similar effects were found for a few other stars, although this example was the most pronounced. The quantitative abundance analysis of HD 169142 (Section 4.4) confirms that Mg is depleted in the photosphere of this star.

4.2 Modelling

Following the inference that some elements were depleted in the photospheres of our programme stars, a more comprehensive abundance analysis was carried out. Initially, solar metallicity model atmospheres were computed under the assumption of local thermodynamic equilibrium (LTE) for adopted values of $T_{\rm eff}$ and log g (initially from Gray & Corbally 1994 and Allen 1973 respectively) using Kurucz's code ATLAS6 (Kurucz 1979). Abundances were then determined by fitting the observations with LTE synthetic spectra calculated using the model atmosphere and spectrum synthesis code UCLSYN (Smith 1992). This interactive program uses atomic data from Kurucz (1995) and also accounts for parameters such as $v \sin i$ values, radial velocity, microturbulence (ξ), temperature ($T_{\rm eff}$), log g and the instrumental profile width. The van der Waals damping constant is treated as temperature and density dependent by the program and is calculated using the asymptotic dipole–dipole (Lindholm–Foley) theory. In this work the very strongest lines have been omitted from the abundance calculations due to the line-blending effects and their relative insensitivity to subtle changes in abundance. Figs 4 and 5 show examples of our modelling. Fig. 4 shows the four spectral regions used in the abundance analysis of the program stars, for the particular case of HD 142666. Fig. 5 shows one of these spectral regions for four of the stars that were modelled. It should be noted that these are LTE models. It is quite possible that NLTE effects could affect the results, but it is very difficult to predict how and by how much the results will change without conducting a full NLTE analysis and making a comparison. Rentzsch-Holm (1996) calculated NLTE abundance corrections of iron and carbon in A-type stars. She found that corrections for iron are always positive over the effective temperature range 7000 to 12 000 K and the log g range 3.5 to 4.5. For the temperature of the stars considered in this paper, the correction did not amount to more than 0.2 dex. For carbon, the corrections were always negative over the range of temperatures and gravities considered here, and were generally small for lines whose equivalent width was below 100 mÅ. Such small changes would not affect the overall conclusions of this paper. However, when making comparisions between the results of this work and those of others, it should be remembered that NLTE effects are not considered here.

For the four stars shown in Fig. 5 the effective temperature and microturbulence could be calculated simultaneously, giving us independent values for these parameters. UCLSYN contains a facility based on the work of Magain (1984) designed to determine the mictroturbulence (ξ), based on an assigned effective temperature

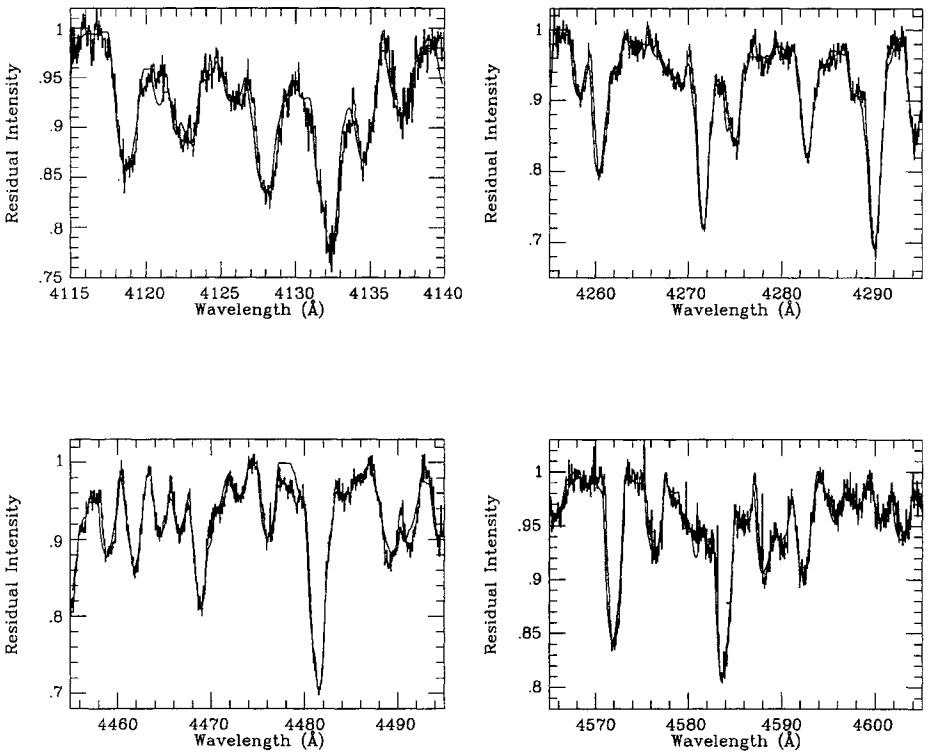

Figure 4. Four different regions of the spectrum of HD 142666 that were used for its abundance analysis. The smooth line shows the model fit to the data (see text).

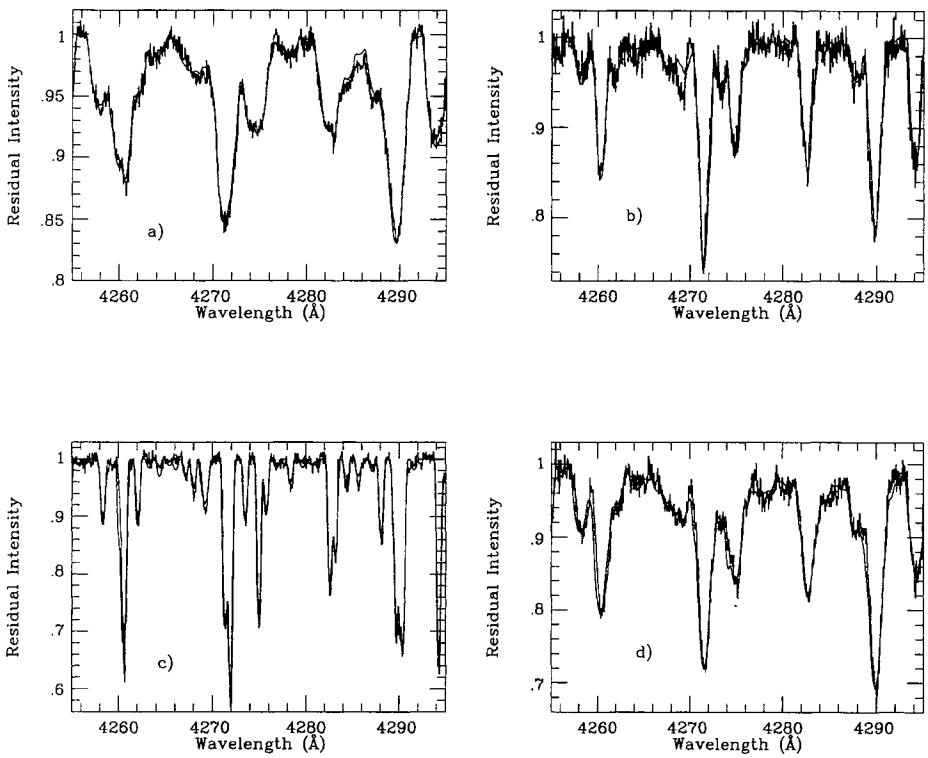

Figure 5. Examples of the same spectral region for four different stars, together with the model fits (smooth lines). Note the more complex spectra as the stars become cooler, and the blending of lines for the higher $v \sin i$ values. (a) HD 216956 (A3V), (b) HD 169142 (A5Ve), (c) HD 139614 (A7Ve) and (d) HD 142666 (A8Ve).

Table 5. Derived parameters for the programme stars.

Star HD	SAO	Name	Sp[1]	$T_{\rm eff}$[2] (K)	$\log g$[3]	ξ[4] (kms^{-1})	$v \sin i$[5] (kms^{-1})	$V_\odot$[5] (kms^{-1})	D[6] (pc)
23362	111388		K2V	5010	4.5	(1)	–	–	6.5[a]
35187	77144		A2/3 IV/Ve	8990	4.1	(3)	93±5	−17±14	202[a]
98800	179815		K5Ve	4510	4.5	(1)	11	12.5±0.4	17[a]
123160	158350		G5V	5570	4.5	(1)	9±1	−6.4±0.4	15.7[a]
135344	206462		F4Ve	6660	4.3	(3)	69±3	−3±3	84[a]
139614	226057		A7Ve	8250†	4.2‡	4.0*	24±1	3±1	157[a]
141569	140789		A0Ve	10040	4.1	(3)	236±9	−6±5	207[c]
142666	183956		A8Ve	7150†	4.4‡	3.0*	70±2	3±1	114[a]
143006	183986		G5Ve	5570	4.5	(1)	12±2	−0.9±0.3	82[a]
144432	184124		A9/F0Ve	7400	4.3	(3)	74±2	2±2	119[a]
158643	185470	51 Oph	B9.5Ve	10480	4.1	(3)	267±5	−20±3	25[c]
161868	122754	γ Oph	A0V	10040	4.1	(3)	214±3	−19±3	29[b]
169142	186777		A5Ve	8400†	4.2‡	3.7*	55±2	−3±2	145[a]
216956	191524	α PsA	A3V	8500†	4.1‡	4.9*	88±2	7±2	8.5[d]

Notes to Table 5.

[1]See Table 1.
[2]Effective temperatures are taken from the spectral type versus effective temperature calibration of Gray & Corbally (1994), except those marked with † which were derived from this work (see Section 4.3).
[3]Values taken from Allen (1973) as those expected for the spectral type except ‡, derived from this work.
[4]Values in brackets have been assumed to be 3 km s^{-1} for A-type stars and 1 km s^{-1} for the later type stars. *This work.
[5]This work. The heliocentric velocity and $v \sin i$ listed for HD 98800 were taken from Fekel & Bopp (1993).
[6][a]Sylvester et al. (1996), [b]Welsh et al. (1994), [c]van Atlana, Lee & Hoffleit (1991), [d]calculated using the M_V and $(B-V)$ tabulated by Oudmaijer et al. (1992).

and the measurement of many weak lines of a particular ionization stage of a single element, using a null-correlation method (i.e. no correlation between abundances and equivalent widths). From this program 'best-fitting' values for ξ and $\log A(X)$ can be calculated, where X is the element under consideration. These values are obviously dependent on the adopted effective temperature, but we found that by carrying out the same procedure for a different ionization stage of the same element (in this case Fe I and Fe II), we could constrain the values of $T_{\rm eff}$, ξ and $\log A(X)$ by altering the temperature until the derived values of ξ and $\log A(X)$ from both ionization stages agree. Obviously, this method relies on the accuracy of the model atmospheres used; uncertainties in the models, gravities and other factors may account for the difference in the temperatures we found for the A7 and A8 stars compared with those expected for the spectral type as tabulated by Gray & Corbally (1994). This process was found to be too difficult to perform accurately for stars of high $v \sin i$ (>100 km s^{-1}), for which unblended lines of a single species were almost impossible to find.

As well as determining the values of $T_{\rm eff}$, ξ and $\log A(X)$, the program also allowed us to obtain measurements of $v \sin i$ and the radial velocity of the programme stars. Table 5 lists these data.

4.3 Derived parameters and sources of error

Abundance analyses were carried out for all of the A-type stars in our sample with the exception of HD 35187 (the data were lower resolution and poorer quality), HD 144432 (this was the coolest star in our A-type sample [A9/F0Ve], and had too many heavily blended lines for a meaningful analysis to be made) and 51 Oph, whose $v \sin i$ was too high for analysis. For the majority of our stars, effective temperatures were adopted from the spectral type versus effective temperature relation of Gray & Corbally (1994), although values of $T_{\rm eff}$ and the microturbulence were derived from the ionization balance modelling in this paper for four stars (HD 139614, 142666, 169142 and 216956, see Table 5). In the case of the remaining stars, values of the microturbulence were simply unavailable. When this was the case, we adopted a microturbulence of 3 km s^{-1} (as a representative average, from VL90) for the A-type stars and 1 km s^{-1} for the later type stars (from Pallavicini, Cerruti-Sola & Duncan 1987). Fig. 6 demonstrates the effect that variations in the microturbulence and effective

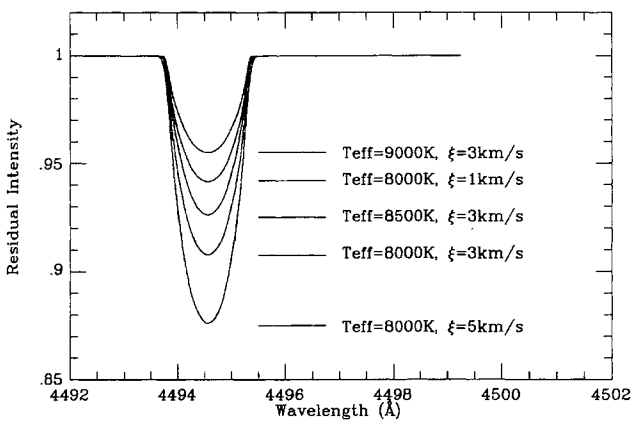

Figure 6. Synthetic models for the Fe I λ4494.56 line using different values of $T_{\rm eff}$ and microturbulence. The $v \sin i$ values of the models remained constant.

Table 6. Derived iron abundances for various values of the microturbulence (ξ) and effective temperature ($T_{\rm eff}$), using a representative line of Fe I at λ4494. Abundances are in dex, with 7.54 being the adopted solar abundance of iron (Biémont et al. 1991).

ξ (km s^{-1})	$T_{\rm eff}$(K) 8000	8500	9000
0	7.54	7.54	7.54
1	7.30	7.40	7.48
3	6.95	7.17	7.35
5	6.85	7.10	7.31

temperature have on the synthetic models produced. The representative line used was Fe I λ4494.56 Å. Models were produced for combinations using effective temperatures of 8000, 8500 and 9000 K, and microturbulences of 0, 1, 3 and 5 km s^{-1}. For each effective temperature, a solar iron abundance (7.54 dex: Biémont et al. 1991) was assumed when $\xi = 0$ km s^{-1}, and the microturbulence altered to observe the effect on the abundance derived from the line. The effects on the derived iron abundance as a function of the adopted microturbulence are listed in Table 6. Similar effects were also found using a representative line of Fe II at λ4491.41.

Other possible sources of error are the log gf values used in the program. The values used by UCLSYN are from CD23 of Kurucz (1995) which are taken mainly from the list of Kurucz (1988) with additions and replacements where more accurate data were available. However, there will always be the possibility of errors or inaccuracies in the data. The propagation of these errors and others from data used by the program obviously cannot be traced and calculated directly, and therefore will lead to errors on the derived effective temperatures and gravities which are unknown. Varying the derived log g and $T_{\rm eff}$ values gave typical variations in abundance of up to 0.2 dex for changes in $T_{\rm eff}$ of 200 K, or for a change in log g between 4.0 and 4.5.

Another significant source of error in our analysis is estimated to result from uncertainties in the placement of the continuum during the normalization of our spectra. Fig. 7 highlights the problem of incorrect normalization. Here the model was kept constant in the two frames to show the potential discrepancy due to a poor continuum placement. This becomes a particularly serious problem for stars with a high $v \sin i$ and for cooler stars which have many lines blended together, giving the appearance of a lower continuum level. This is particularly troublesome in the short, curved-continuum orders in an echelle spectrum. Many authors have commented on the difficulty of continuum placement (e.g. Stürenburg 1993; Hill 1995), which is an important factor in abundance analyses such as these.

When determining the correct continuum placement for our spectra, UCLSYN was used to calculate a solar abundance model using appropriate stellar parameters for the star being analysed. The solar model showed where the continuum ought to be reached, which was used as a guide to normalize the observed spectrum correctly. This method was found to yield satisfactory results for all the stars analysed. In determining the error associated with continuum placement, the observed spectrum was inspected and two 'extremes' of normalization were made, one too high, one too low. Abundances from an individual line were calculated for both extremes, and half the difference between the two values was

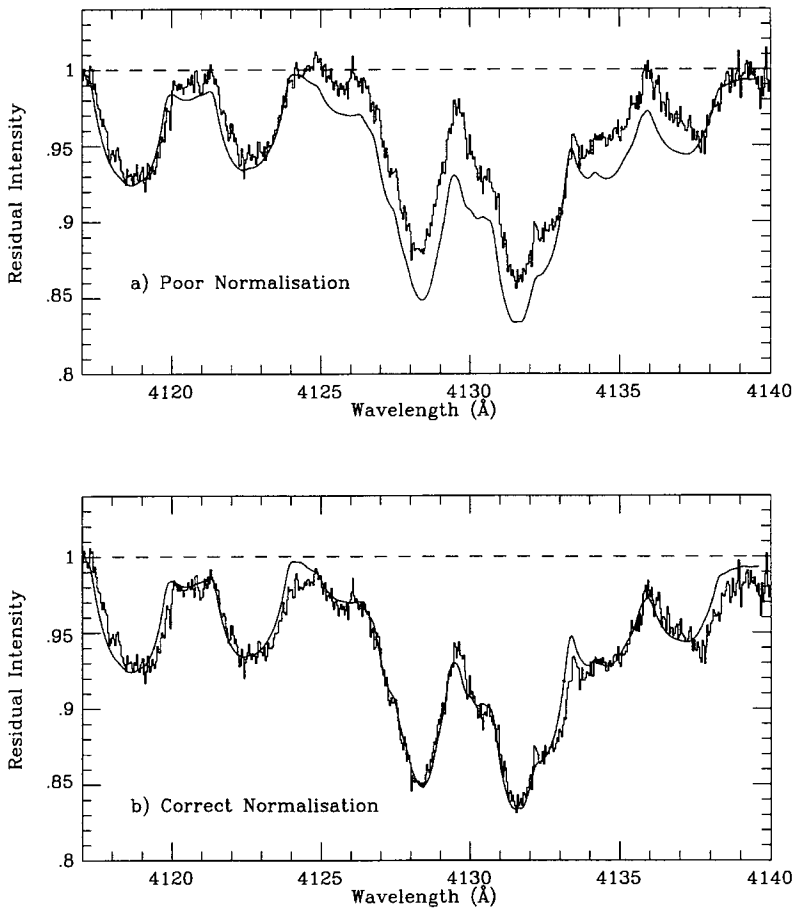

Figure 7. The effects of continuum placement on the fit. The lower continuum placement in (a) results in a relatively poor fit to the stronger lines whereas the higher continuum placement in (b) produces a good fit to both the weaker and the stronger lines. The correction is not simply first order (i.e. a linear correction), but a higher order effect, requiring greater care to remove. The synthetic model (smooth line) is identical in both cases.

Table 7. Derived abundances. Each entry indicates the logarithmic abundance of the element, relative to the solar values listed in the final column (the solar values are on a scale where $H = 12.00$). The numbers in parentheses to the right of each abundance entry represent the number of lines used in the analysis of that element.

	Star(HD)								
	141569	161868	216956	169142	139614	142666	29 Cyg	Vega	Sun
	A0Ve	A0V	A3V	A5Ve	A7Ve	A8Ve	A0p	A0V	G2V
C	–	–	−0.19 (2)	−0.05 (2)	−0.07 (2)	+0.15 (3)	−0.28	−0.18	8.60[1]
Mg	0.00 (3)	−0.33 (4)	0.00 (1)	−0.56 (4)	−0.08 (3)	−0.21 (2)	−1.73	−0.84	7.58
Si	–	–	−0.05 (2)	−0.86 (2)	−0.52 (2)	–	–	–	7.55
S	–	–	+0.05 (3)	–	−0.12 (3)	−0.12 (3)	−0.23	0.00	7.21
Ca	0.00 (2)	–	−0.13 (3)	−0.23 (8)	−0.33 (6)	−0.24 (7)	−1.18	−0.44	6.36
Ti	+0.14 (2)	−0.16 (4)	−0.09 (3)	−0.34 (5)	−0.21 (8)	−0.13 (12)	−1.41	−0.45	4.99
Cr	–	–	+0.04 (5)	−0.17 (8)	−0.11 (9)	−0.13 (11)	–	–	5.67
Mn	–	–	−0.03 (3)	−0.24 (8)	–	−0.22 (4)	–	–	5.39
Fe	+0.03 (2)	−0.21 (4)	−0.03 (>20)	−0.11 (>20)	−0.16 (>30)	−0.03 (>30)	−1.67	−0.62	7.54[2]
Co	–	–	–	+0.12 (2)	–	−0.14 (2)	–	–	4.90
Ni	–	–	+0.02 (2)	−0.13 (2)	−0.07 (2)	−0.44 (3)	–	–	6.25
Average*	0.04	−0.23	−0.02	−0.18	−0.17	−0.06			

Note. All solar abundances taken from Anders & Grevesse (1989) except [1]Grevesse (1991) and [2]Biémont et al. (1991).
*Average metallicity values. These averages do not include Si and Mg in the case of HD 169142 or Si in the case of HD 139614, for which significant underabundances are found. See text for details.

taken as the error on the abundance measurement. The adopted abundance was taken as that derived from the correctly normalized spectrum. The exception to the above discussion of error determination is HD 139614, whose $v \sin i$ of 24 km s^{-1} was low enough to reveal the true continuum in the observed spectrum. The errors for this star (from the allowed variations of the model that still maintained a good fit to the profiles) were found to be less than those for the other stars.

Each elemental abundance, as tabulated in Table 7, is a logarithmic average of all the individual abundances derived from fits to four different spectral regions. Incorporating all of the above sources of error, we estimate that the abundances tabulated in Table 7 will have errors of up to ± 0.15 dex.

4.4 Abundances and their implications

When determining the abundance of a particular element in a star, the values obtained from several lines in different echelle orders were considered. Those that were deemed to be too weak for accurate measurement, or those that were severely blended with other and stronger lines were not included in the final calculation. Several elements (Fe, Mg, Mn, Ti, Cr, Ca) had lines from more than one ionization stage that could be analysed. Some elements, such as those of carbon, sulphur, cobalt and nickel, had very few lines that could be modelled accurately. The abundances of these elements are therefore the least accurate of those derived. Oxygen was not included in the analysis due to the lack of suitable lines. Although the O I triplet at λ7774 was covered in our spectra, the data were affected by fringing effects from one of the optical elements (Ryan 1995) which could not be removed during the processing of the spectra. The final abundance, relative to solar, listed for each element in Table 7 is an average from all the lines considered acceptable for analysis. The number of lines used to derive the abundance of each element is given in parentheses. Table 7 also lists abundances, again relative to solar, for Vega (considered to be a mild λ Boötis star: VL90) and for a true λ Boötis star, 29 Cyg (again taken from VL90). The final column of Table 7 lists the adjusted solar abundances [from Anders & Grevesse (1989), except where stated], relative to which the abundances of the other stars are given. A dash in Table 7 indicates that an abundance was not derived, usually because of too high a $v \sin i$ or because of severe line blending in the case of the later type stars in the analysis.

For the A3V spectral standard (and Vega-like star) α PsA (HD 216956), the abundances derived for 10 elements are all solar within the uncertainties. In the case of the A0V spectral standard (and Vega-like star) γ Oph (HD 161868) and the A0Ve star HD 141569, abundances could be derived for only three and four elements respectively, because of their high $v \sin i$ values – the abundances are close to solar values in both cases. The abundances of 10 elements in the A8Ve Vega-like star HD 142666 are all within 0.24 dex of solar, apart from Ni, which appears to be 0.4 dex underabundant. The A7Ve Vega-like star HD 139614 exhibits depletions of 0.52 dex in Si and 0.33 dex in Ca but the depletions of other elements are all less than 0.2 dex. The largest depletions in our sample are exhibited by the A5Ve Vega-like star HD 169142, which shows depletions of 0.86 dex in Si and 0.56 dex in Mg, although most of the remaining elements are within 0.25 dex of solar. λ Boötis stars possess typical metal underabundances lying in the range between −0.5 and −2.0 dex of solar (Iliev & Barzova 1995 and references therein), and the relatively high depletions of Mg and Si in HD 169142 and of Si in HD 139614 do fall within this range. A-type stars are known to exhibit a range of abundances, even within the 'normal' A-type star category (Holweger, Gigas & Steffan 1986) and most of the other abundances found here are not in excess of usual variations seen amongst normal A-type dwarf stars. The average stellar metallicities listed in the final row of Table 7 highlight the fact that these Vega-like stars generally exhibit 'normal' metallicities. Venn & Lambert (1990) suggested a link between the depletions in λ Boötis stars and those found in the interstellar medium (ISM). They noted that the pattern of depletion observed in λ Boo stars could be correlated to that seen in the ISM, suggesting that some of the heavy elements in the circumstellar environment of these stars have accreted on to grain surfaces. No similar patterns were found in our sample of Vega-like stars. In view of the significant depletions of Mg and Si in the photosphere of HD 169142, and of Si in HD 139614, it is interesting to note that magnesium and silicon are major constituents of silicate grains, which are likely to be present in the discs of Vega-like stars (Sylvester et al. 1996). The observed photospheric depletions of these elements might be due to their residing in circumstellar silicate grains. HD 169142 indeed exhibits an 18-μm silicate emission feature (Sylvester et al. 1996) while the mid-infrared spectrum of HD 139614 has yet to be measured. However, the absence of any significant depletion of Ca, Ti or Fe in the photospheres of these stars is puzzling, since these elements are normally even more depleted than Mg and Si.

4.5 Relation between abundances and IR excess?

Our programme Vega-like stars have large fractional excess IR luminosities (L_{IR}/L_*). To test whether there is any correlation between depletions and L_{IR}/L_*, we compared the L_{IR}/L_* values of the Vega-like stars in our sample with those of λ Boötis stars having IR excesses. The λ Boötis stars were selected from those listed by King (1994) as having an IR excess. In addition, 29 Cyg (studied by VL90) was also included in the analysis. Table 8 lists the derived values of L_{IR}/L_*. The values for our programme stars were taken from Sylvester et al. (1996), except for α PsA which was taken from Backman & Paresce (1993). For the λ Boötis stars, values for F_*, the stellar flux, were calculated by integrating under a Kurucz model atmosphere, having an effective temperature taken from the spectral

Table 8. Fractional excess IR luminosities (L_{IR}/L_*) of the Vega-like stars in our abundance analysis, and of some λ Boötis stars for comparison.

HD	SAO	Name	Type	L_{IR}/L_*
39060	234134	β Pic	A5V	2.6×10^{-3}
139614	226057		A7Ve	0.39
141569	140789		A0Ve	8.4×10^{-3}
142666	183956		A8Ve	0.34
161868	122754	γ Oph	A0V	4.2×10^{-5}
169142	186777		A5Ve	0.088
172167	67174	Vega	A0V	2.3×10^{-5}
216956	191524	α PsA	A3V	8×10^{-5}
λ Boötis Stars				
31295	94201	π^1 Ori	A2V	7.4×10^{-5}
111604	63217		A3V	4.7×10^{-4}
125162	44965	λ Boo	A0V	2.6×10^{-5}
150177	141298		F3V	1.5×10^{-3}
188728	105438	ϕ Aql	A1IV	2.0×10^{-4}
192640	69674	29 Cyg	A0p	1.4×10^{-3}

type versus $T_{\rm eff}$ calibration of Gray & Corbally (1994), normalized to the dereddened U, B and V photometric fluxes. Values of $F_{\rm IR}$, the observed IR excess flux, were derived by integrating under smooth curves fitted to the *IRAS* photometric fluxes, after subtraction of the optically normalized stellar photospheric energy distributions.

The $L_{\rm IR}/L_*$ ($\equiv F_{\rm IR}/F_*$) values of the λ Boötis stars are in the range 3×10^{-5} to 1.5×10^{-3}, towards the bottom end of the range shown by Vega-like stars. However, the possession of a value of $L_{\rm IR}/L_*$ in this range by an A-type Vega-like star does not guarantee the presence of λ Boötis-type photospheric abundances – α PsA and γ Oph (this paper) and β Pic (Holweger & Rentzsch-Holm 1995) all have $L_{\rm IR}/L_*$ in this range but exhibit solar abundance distributions. It is not clear how this can be explained in terms of the accretion hypothesis, except by postulating that the accretion of depleted circumstellar gas has not occurred in the case of the latter stars.

The lack of pronounced photospheric depletions for those Vega-like stars in our sample with large values of $L_{\rm IR}/L_*$ could be due to the fact that they are all emission-line stars (Paper II) – mass outflows from these stars may prevent the accretion of circumstellar gas or, if depleted circumstellar gas has been accreted, the mass motions may prevent the formation of a thin, stable layer with abnormal abundances at the top of the photosphere such as is hypothesized to be needed for the λ Boötis phenomenon to be observed. It is interesting to note that HD 139614 and 169142, the two stars showing Si depletions have the lowest $v \sin i$ values (24 and 55 km s^{-1} respectively: Table 5) amongst the six A-type stars for which abundances have been derived. These two Ae stars also exhibit single-peaked Balmer emission-line profiles, while the other two Ae stars in Table 7 exhibit (1) no Hα emission (HD 216956, an MK standard) and (2) a highly asymmetric double-peaked profile (HD 142666, see Paper II). The low $v \sin i$ values and single-peaked emission profiles of HD 139614 and 169142 suggest that they may be being seen closer to pole-on than is the case for the other stars, although whether this is related to the fact that they show Si and Mg depletions is not clear.

5 CONCLUSIONS

This is the first of two papers analysing high-resolution spectroscopy of Vega-like stars, and considers the effective temperatures and gravities of the stars and their photospheric abundances. Paper II considers the ages of the stars from their emission-line characteristics and lithium abundances. Circumstellar and interstellar absorption lines are also analysed there.

In the current paper, of the 13 Vega-like stars studied, four were noted to have significantly different spectral types from those previously published in the literature. The resultant changes in adopted effective temperature for the stars are the following: HD 2623 (M2III): 1800 K lower than before (and a different luminosity class also); HD 123160 (G5V): 1000 K higher; HD 135344 (F4Ve): over 3000 K lower (also noted by Oudmaijer et al. 1992, Zuckerman et al. 1995 and Coulson & Walther 1995); HD 169142 (A5Ve): 2500 K lower. Radial velocities and $v \sin i$ values have been derived for almost all the stars in the sample. For four of the lower $v \sin i$ A-type stars in the sample, effective temperatures and surface gravities were derived directly from spectral synthesis modelling.

The photospheric abundances of 10 elements were derived for the four A-type dwarf stars with low $v \sin i$ values (and for three elements for two other stars with higher $v \sin i$ values). The mean elemental underabundance relative to solar for the six stars was only 0.1 dex which is no more than typical variations seen in 'normal' A-type stars (Holweger et al. 1986). No underabundances as high as those seen in the metal-depleted λ Boo class of stars (0.5–2 dex) were found in our sample, apart from Si and Mg in HD 169142 which were 0.86 and 0.56 dex underabundant respectively, and Si in HD 139614 which was 0.52 dex underabundant relative to solar values. If we follow the accretion hypothesis of Venn & Lambert (1990) for the underabundances of the λ Boo stars, our results would suggest that Mg and Si in these two stars have become locked up in grains in the circumstellar environment. A silicate feature has been observed at 18 μm in the spectrum of HD 169142, strengthening this hypothesis. However, the reason for the absence of significant depletions in these stars of other refractory elements, such as Ca, Fe and Ti which should also be locked up in silicate grains, remains unclear.

ACKNOWLEDGMENTS

We would like to thank Dr Francisco Diego for obtaining the spectra of HD 2623, 23362 and 35187 during the commissioning run of the ROESC echelle spectrograph at the Observatorio Astronomico Nacional, Mexico. We would also like to thank Dr K. Smith for suggesting improvements to the original manuscript and for advice and assistance in using the UCLSYN program, and also Dr R. Sylvester for help in obtaining the $L_{\rm IR}/L_*$ values for the stars. The spectra were analysed using the computing facilities of the Starlink node at University College London. Starlink is funded by the Particle Physics and Astronomy Research Council, UK. The work also used the IRAF data reduction package, distributed by the National Optical Astronomy Observatories, which is operated by the Association of Universities for Research in Astronomy, Inc., under contract to the National Science Foundation. Use was made of the SIMBAD data base, operated at the CDS, Strasbourg, France. We thank the referee for helpful comments.

REFERENCES

Abt H. A., Meinel A. B., Morgan W. W., Tapscott J. W., 1968, An Atlas of Low-Dispersion Grating Spectra
Allen C. W., 1973, Astrophysical Quantities. 3rd edn. Athlone Press, London
Allen L. E., Strom K. S., 1995, AJ, 109, 1379
Anders E., Grevesse N., 1989, Geochim. Cosmochim. Acta, 53, 197
Andrillat Y., Jaschek M., Jaschek C., 1990, A&A, 233, 474
Aumann H. H., 1985, PASP, 97, 885
Aumann H. H. et al., 1984, ApJ, 278, L23
Backman D. E., Paresce F., 1993, in Levy E. H., Lunine J. I., eds, Protostars & Planets III. Univ. of Arizona, Tucson, p. 1253
Baschek B., Slettebak A., 1988, A&A, 207, 112
Biémont E., Baudoux M., Kurucz R. L., Ansbacher W., Pinnington E. H., 1991, A&A, 249, 539
Charbonneau P., 1991, ApJ, 372, L33
Coulson I. M., Walther D. M., 1995, MNRAS, 274, 977
Danks A. C., Dennefeld M., 1994, PASP, 106, 382
Dunkin S. K., Barlow M. J., Ryan S. G., 1997, MNRAS, submitted
Fekel F. C., Bopp B. W., 1993, ApJ, 419, L89
Gillett F. C., 1986, in Israel F. P., ed., Light on Dark Matter. Reidel, Dordrecht, p.61
Gray R. O., 1988, AJ, 95, 220
Gray R. O., Corbally C. J., 1994, AJ, 107, 742
Gray D. F., Garrison R. F., 1987, ApJS, 65, 581
Gray D. F., Garrison R. F., 1989a, ApJS, 69, 301
Gray D. F., Garrison R. F., 1989b, ApJS, 70, 623
Grevesse N., 1991, in Michaud G., Tutukov A., eds, Proc. IAU Symp. 145, Evolution of Stars: The Photospheric Abundance Connection. Kluwer, Dordecht, p. 63

Hauck B., Mermilliod M., 1990, A&AS, 86, 107
Hill G. M., 1995, A&A, 294, 536
Hoffleit D., Jashek C., 1982, The Bright Star Catalogue. Yale Univ. Observatory, New Haven
Holweger H., Rentzsch-Holm I., 1995, A&A, 303, 819
Holweger H., Gigas D., Steffen M., 1986, A&A, 155, 58
Houk N., 1978, Michigan Catalogue of Two-Dimensional Spectral Types for the HD stars, Vol 2. Univ. of Michigan, Ann Arbor
Houk N., 1982, Michigan Catalogue of Two-Dimensional Spectral Types for the HD stars, Vol 3. Univ. of Michigan, Ann Arbor
Houk N., 1988, Michigan Catalogue of Two-Dimensional Spectral Types for the HD stars, Vol 4. Univ. of Michigan, Ann Arbor
Howarth I. D., Murray J., 1988, Starlink User Note, No. 50
Iliev I., Barzova I. S., 1995, A&A, 302, 735
Jaschek C., Jaschek M., 1990, The Classification of Stars. Cambridge Univ. Press, Cambridge
Johnson H. L., Morgan W. W., 1953, ApJ, 117, 313
King J. R., 1994, MNRAS, 269, 209
Kirkpatrick J. D., Henry T. D., McCarthy D. W., Jr, 1991, ApJS, 77, 417
Kurucz R. L., 1979, Dudley Obs. Rep., No. 14, p. 271
Kurucz R. L., 1988, in McNally D., ed., Trans. IAU, XXB. Kluwer, Dordrecht, p. 168
Kurucz R. L., 1995, ASP Conf. Ser. 78. Astron. Soc. Pac., San Francisco, p. 205
Magain P., 1984, A&A, 134, 189
Michaud G., Charland Y., 1986, ApJ, 311, 326
Morgan W. W., Keenan P. C., 1973, ARA&A, 11, 29
Morgan W. W., Keenan P., Kellman E., 1943, An Atlas of Stellar Spectra. Univ. of Chicago Press, Chicago
Morgan W. W., Abt H. A., Tapscott J. W., 1978, Revised MK Spectral Class for Stars Earlier than the Sun. Yerkes Observatory, Wisconsin
Oudmaijer R. D., van der Veen W. E. C. J., Waters L. B. F. M., Trams N. R., Waelkens C., Engelsman E., 1992, A&AS, 96, 625
Pallavicini R., Cerruti-Sola M., Duncan D. K., 1987, A&A, 174, 116
Rentzsch-Holm I., 1996, A&A, 312, 966
Ryan S. G., 1995, AAO Newsletter, January, p.13
Schmidt-Kaler T. H., 1982, in Schaifers K., Voigt H. H., eds, Landolt-Börnstein New Series, Astronomy and Astrophysics, Stars and Star Clusters, Vol. 2b. Springer-Verlag
Smith K. C., 1992, PhD Thesis, Univ. of London, Chapter 5
Sneden C., 1973, PhD Thesis, Univ. of Texas at Austin
Stencel R. E., Backman D. E., 1991, ApJS, 75, 905
Stürenburg S., 1993, A&A, 277, 139
Sylvester R. J., Barlow M. J., Skinner C. J., 1992, in Gondhalekar P. M., ed., Proc. Workshop Astronomy and Astrophysics, Dusty Discs. RAL Report 92-084, p. 172
Sylvester R. J., Skinner C. J., Barlow M. J., Mannings V., 1996, MNRAS, 279, 915
Torres-Dogden A. V., Weaver W. B., 1993, PASP, 105, 639
van Atlana W. F., Lee J., Hoffleit D., 1991, New Yale General Catalogue of Trigonometric Stellar Parallaxes. Yale Univ. Observatory, New Haven
van der Veen W. E. C. J., Trams N. R., Waters L. B. F. M., 1993, A&A, 269, 231
Venn K. A., Lambert D. L., 1990, ApJ, 363, 234 (VL90)
Walker H. J., Wolstencroft R. D., 1988, PASP, 100, 1509
Waters L. B. F. M., Trams N. R., Waelkens C., 1992, A&A, 262, L37
Welsh B. Y., Craig N., Vedder P. W., Vallerga J. V., 1994, ApJ, 437, 638
Whitelock P. A., Menzies J. W., Catchpole R. M., Feast M. W., Roberts G., Marang F., 1991, MNRAS, 250, 638
Zuckerman B., Forveille T., Kastner J. H., 1995, Nat, 373, 494

This paper has been typeset from a T_EX/L^AT_EX file prepared by the author.